arXiv:cond-mat/0506237v2 [cond-mat.supr-con] 17 Jun 2005

Downward Shift of Infrared Conductivity Spectral Weight at the DDW Transition: Role of Anisotropy

Rouzbeh Gerami and Chetan Nayak
Department of Physics, University of California, Los Angeles, California 90095–1547

(Dated: February 2, 2008)

We consider the motion of conductivity spectral weight at a finite-temperature phase transition at which $d_{x^2-y^2}$ density-wave (DDW) order develops. We show that there is a shift of spectral weight to higher frequencies if the quasiparticle lifetime is assumed to be isotropic, but a shift to lower frequencies if the quasiparticle lifetime is assumed to be anisotropic. We suggest that this is consistent with recent experiments on the pseudogap phase of the cuprate superconductors and, therefore, conclude that the observation of a downward shift in the spectral weight at the pseudogap temperature does not militate against the DDW theory of the pseudogap.

PACS numbers: 74.72.-h, 74.25.Gz

I. INTRODUCTION

It has been proposed[1] that the anomalous behaviors observed in the pseudogap phase of the underdoped cuprates can be explained by assuming the existence of a new long-range ordered density-wave with $d_{x^2-y^2}$ symmetry (DDW)[2] which competes with superconducting order. As a result of this order, the excitation spectrum acquires a partial gap with the same symmetry and structure as the gap observed in the pseudogap state. The DDW theory has been applied to explain several observed anomalies in the pseudogap phase of the cuprates[3,4,5,6,7,8,9]. Attempts to directly observe it in neutron scattering are encouraging[10].

One of the arguments against the DDW theory is that it is inconsistent with in-plane optical conductivity measurements. The assumption has been that as the temperature is reduced below the pseudogap transition temperature T^*, and a (partial) gap opens, some of the low-energy excitations are lost and this should cause a reduction in the low-frequency optical conductivity, which is compensated by an increase in the spectral weight at higher frequencies. Such behavior is seen in some charge density-wave systems[11], but is not observed in the cuprates[12,13,14], which might be taken as an indication that the pseudogap is associated with superconducting fluctuations, which would cause a downward motion of spectral weight (which would eventually coalesce into a zero-frequency δ-function in the superconducting state).

These experiments find no changes in the in-plane spectral weight within their error bars[12,13,14]: spectral weight lost at the low-energy end of the measured frequency range appears (perhaps unexpectedly) at very low frequencies, and hence accompanies a narrowing of the low-energy optical conductivity peak. This phenomenon was interpreted in ref. 12 as the lack of any in-plane optical evidence for the pseudogap.

In this paper we show how the DDW theory of the pseudogap can be consistent with this observed effect. The key to this phenomenon, we believe, (as conjectured in 12) is the strong anisotropy in the quasiparticle spectrum and scattering rate in the cuprates. ARPES experiments clearly show that quasiparticles in the antinodal region of the Brillouin zone ($(k_x, k_y) \sim (0, \pm\pi), (\pm\pi, 0)$), where the gap opens in the pseudogap phase, scatter much more strongly than they do in the nodal region ($(k_x, k_y) \sim (\pm\pi, \pm\pi)$), where the gap is zero. (While the transport lifetime is not the same as the quasiparticle lifetime observed in ARPES, we assume that it has a similar anisotropy, as in "hot spot" and "cold spot" theories[16,17].) The lost carriers, therefore, give a relatively small contribution to the conductivity. The loss of these carriers can be cancelled by a general reduction of all the scattering rates, as the temperature is reduced. As pointed out in ref. 15, this may also explain the observed behavior in several classes of spin-density-wave (SDW) and CDW systems.

These ideas are borne out by a model calculation with the mean-field DDW Hamiltonian and an *ansatz* for the quasiparticle lifetime. We show that when the lifetime has an anisotropic form motivated by ARPES measurements, the conductivity spectral weight shifts downward, as in the cuprates. However, for an isotropic lifetime, the spectral weight shifts upward.

II. MEAN-FIELD HAMILTONIAN

The mean-field Hamiltonian for the DDW state is

$$H_{\rm DDW} = \sum_{\mathbf{k},\sigma} [(\epsilon_{\mathbf{k}} - \mu) c^\dagger_{\mathbf{k}\sigma} c_{\mathbf{k}\sigma} + (i\Delta_{\mathbf{k}} c^\dagger_{\mathbf{k}\sigma} c_{\mathbf{k}+\mathbf{Q}\sigma} + \text{h.c.})] \quad (1)$$

where $c_{\mathbf{k}}$ is the annihilation operator of an electron in a state with momentum $\mathbf{k}$ and spin σ, μ is the chemical potential, $\Delta_{\mathbf{k}} = \langle c^\dagger_{\mathbf{k}\sigma} c_{\mathbf{k}+\mathbf{Q}\sigma} \rangle = \Delta_0(\cos k_x - \cos k_y)/2$ is the DDW order parameter and $\mathbf{Q} = (\pi, \pi)$ is the DDW ordering wave vector, with lattice spacing set to unity. The tight-binding band structure is given by $\epsilon_{\mathbf{k}} = \epsilon_{1\mathbf{k}} + \epsilon_{2\mathbf{k}}$, with

$$\epsilon_{1\mathbf{k}} = -2t(\cos k_x + \cos k_y)\,, \quad \epsilon_{2\mathbf{k}} = 4t' \cos k_x \cos k_y. \quad (2)$$

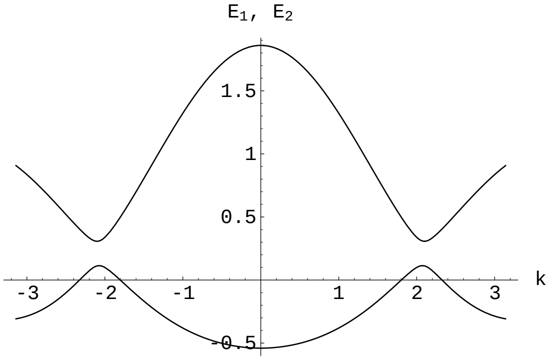

FIG. 1: DDW quasiparticle energy bands along the line $k_y = k_x/2$ in the Brillouin zone for $t = 0.3, t' = 0.09, \Delta_0 = 0.2$ and $\mu = -0.3$ eV.

where t and t' are nearest-neighbor and next-neighbor hopping parameters.

Introducing the two-component field operator $\chi^\dagger_{\mathbf{k}\sigma} = \begin{pmatrix} c^\dagger_{\mathbf{k}\sigma} & -ic^\dagger_{\mathbf{k+Q}\sigma} \end{pmatrix}$ the mean field Hamiltonian can be written as

$$H_{DDW} = \sum_{\mathbf{k},\sigma} \chi^\dagger_{\mathbf{k}\sigma} B_{\mathbf{k}} \chi_{\mathbf{k}\sigma} \tag{3}$$

with

$$B_{\mathbf{k}} = \begin{pmatrix} \epsilon_{\mathbf{k}} - \mu & \Delta_{\mathbf{k}} \\ \Delta_{\mathbf{k}} & \epsilon_{\mathbf{k+Q}} - \mu \end{pmatrix} \tag{4}$$

or

$$B_{\mathbf{k}} = (\epsilon_{2\mathbf{k}} - \mu) + \epsilon_{1\mathbf{k}}\sigma^3 + \Delta_{\mathbf{k}}\sigma^1 \tag{5}$$

where σ^i are the Pauli matrices and the sum is over half the original Brillouin zone (reduced Brillouin zone - RBZ), *i.e.* $|k_x| + |k_y| \leq \pi$, .

Diagonalizing the Hamiltonian will then give the DDW quasiparticle energy bands

$$E_{1,2} = (\epsilon_{2\mathbf{k}} - \mu) \pm \sqrt{\epsilon^2_{1\mathbf{k}} + \Delta^2_{\mathbf{k}}} \tag{6}$$

as depicted in figure 1.

III. GREEN FUNCTION

The "non-interacting" Nambu Green's function can then be obtained by inverting the matrix $B_{\mathbf{k}}$. (For now, the only relevant interactions are the electron-electron interactions which generate the DDW coupling. All other interactions including quasiparticle-quasiparticle and quasiparticle-impurity interactions will be taken into account later by assuming a non-zero self energy).

The 2×2 Nambu Green function is defined by

$$\begin{aligned} G_0(\mathbf{k}, t) &= \langle T \chi_{\mathbf{k}}(t) \chi^\dagger_{\mathbf{k}}(0) \rangle \\ &= \begin{pmatrix} \langle T c_{\mathbf{k}}(t) c^\dagger_{\mathbf{k}}(0) \rangle & i \langle T c_{\mathbf{k}}(t) c^\dagger_{\mathbf{k+Q}}(0) \rangle \\ -i \langle T c_{\mathbf{k+Q}}(t) c^\dagger_{\mathbf{k}}(0) \rangle & \langle T c_{\mathbf{k+Q}}(t) c^\dagger_{\mathbf{k+Q}}(0) \rangle \end{pmatrix} \end{aligned} \tag{7}$$

The Fourier transform of the Green function matrix is then

$$\begin{aligned} G_0(\mathbf{k}, \omega) &= \int dt e^{i\omega t} G_0(\mathbf{k}, t) \\ &= \frac{1}{(\omega + i\delta) - (\epsilon_{2\mathbf{k}} - \mu) - \epsilon_{1\mathbf{k}}\sigma^3 - \Delta_{\mathbf{k}}\sigma^1} \\ &= \frac{(\omega - (\epsilon_{2\mathbf{k}} - \mu) + \epsilon_{1\mathbf{k}}\sigma^3 + \Delta_{\mathbf{k}}\sigma^1}{\omega - (\epsilon_{2\mathbf{k}} - \mu) + i\delta)^2 - \epsilon^2_{1\mathbf{k}} + \Delta^2_{\mathbf{k}}} \end{aligned} \tag{8}$$

We now consider the effects of impurity scattering and 'residual' electron-electron interactions. Here, we will capture their combined effect by introducing a non-zero single-particle self-energy $\Sigma(\mathbf{k}, \omega) = \Sigma_1(\mathbf{k}, \omega) + i\Sigma_2(\mathbf{k}, \omega)$, where the real and imaginary parts give the energy renormalization and quasiparticle lifetime, respectively. Neglecting the shift in the excitation energy due to the real part $\Sigma_1(\mathbf{k}, \omega)$, the self-energy can be written in terms of the quasiparticle lifetime as

$$\Sigma(\mathbf{k}, \omega) = -\frac{i}{\tau(\mathbf{k}, \omega)} \tag{9}$$

where $1/\tau(\mathbf{k}, \omega)$ is the quasiparicle scattering rate (inverse lifetime). Including the self-energy, the full Green's function $G(\mathbf{k}, \omega)$ will then be given according to Dyson's equation by

$$G(\mathbf{k}, \omega) = \left(G_0(\mathbf{k}, \omega)^{-1} - \Sigma(\mathbf{k}, \omega) \right)^{-1} \tag{10}$$

The spectral function $A(\mathbf{k}, \omega)$ can then be calculated by taking the imaginary part of the Green function

$$A(\mathbf{k}, \omega) = -\frac{1}{\pi} \text{Im } G(\mathbf{k}, \omega) = \frac{1}{\pi\tau} \frac{(\omega - \epsilon_{2\mathbf{k}} + \mu)^2 + (\epsilon^2_{1\mathbf{k}} + \Delta^2_{\mathbf{k}}) + (1/\tau)^2 + 2(\omega - \epsilon_{2\mathbf{k}} + \mu)(\epsilon_{1\mathbf{k}}\sigma^3 + \Delta_{\mathbf{k}}\sigma^1)}{[(\omega - E_{1\mathbf{k}})(\omega - E_{2\mathbf{k}}) - (1/\tau)^2]^2 + (2(\omega - \epsilon_{2\mathbf{k}} + \mu)/\tau)^2} \tag{11}$$

In Figure 2, the diagonal elements of the Nambu spectral function matrix $A(\omega, k_x, k_y = 0)$ are plotted against

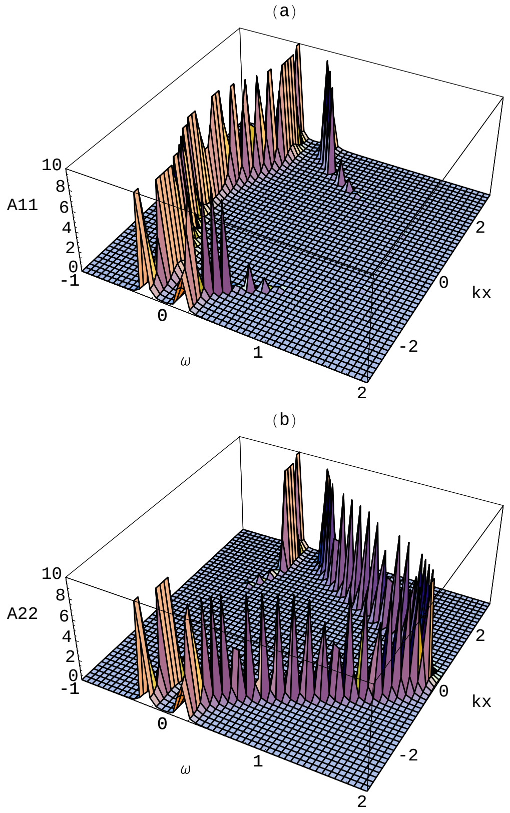

FIG. 2: Elements of the DDW spectral function matrix for $1/\tau = 0.005$ eV: (a)$A_{11}(\omega, k_x, k_y = 0)$ and (b)$A_{22}(\omega, k_x, k_y = 0)$. Other parameters are the same as in figure 1.

k_x and ω. For demonstration purposes, the scattering rate here is assumed to be a constant $1/\tau = 0.02$ eV (independent of momentum and frequency). The diagonal entries A_{11} and A_{22} have peaks centered mostly at energies corresponding to the upper and lower energy bands (E_1 and E_2) respectively.

IV. OPTICAL CONDUCTIVITY

Having found the spectral function $A(\omega, \mathbf{k})$, the real part of the AC conductivity can now be calculated by using the Kubo formula

$$\text{Re}\ \sigma_{xx}(\omega) = \frac{1}{\omega}\text{Im}\ \Pi_{xx}(i\omega_n \rightarrow \omega + i\delta) \tag{12}$$

where $\Pi(i\omega_n)$ is the Fourier tansform of the current-current correlation function in Matsubara formalism

$$\Pi_{xx}(i\omega_n) = \int_0^\beta d\tau e^{i\omega_n \tau}\Pi_{xx}(\tau) \tag{13}$$

with

$$\Pi_{xx}(\tau) = \langle T_\tau j_x(\tau) j_x(0)\rangle \tag{14}$$

The current operator for the DDW quasiparticles can be obtained by minimally-coupling the mean-field Hamiltonian (1) to the electromagnetic field, $\mathbf{A}$, and differentiating once with respect to $\mathbf{A}$:

$$\begin{aligned}\mathbf{j} = \sum_{RBZ}\Big[&\mathbf{v}_{F2}(\mathbf{k})\left(\chi^\dagger_{\mathbf{k}}\chi_{\mathbf{k}}\right) + \mathbf{v}_{F1}(\mathbf{k})\left(\chi^\dagger_{\mathbf{k}}\sigma^3\chi_{\mathbf{k}}\right) \\ &+ \mathbf{v}_{\Delta}(\mathbf{k})\left(\chi^\dagger_{\mathbf{k}}\sigma^1\chi_{\mathbf{k}}\right)\Big]\end{aligned} \tag{15}$$

where $\mathbf{v}_{F1}(\mathbf{k}) = \nabla_{\mathbf{k}}\epsilon_1(\mathbf{k})$,$\mathbf{v}_{F2}(\mathbf{k}) = \nabla_{\mathbf{k}}\epsilon_2(\mathbf{k})$ and $\mathbf{v}_{\Delta}(\mathbf{k}) = \nabla_{\mathbf{k}}\Delta(\mathbf{k})$.

Using this form of the current operator, the current-current correlation function can be written in terms of the elements of the imaginary-time Nambu Green's function $\mathcal{G}_{ij}$ (the non-interacting Green's function G_{ij} is now promoted to the interacting one $\mathcal{G}_{ij}$, to take the effect of the residual interactions into account). We will have

$$\begin{aligned}\langle T_\tau j(\tau) j(0)\rangle = -\sum_{RBZ}&\Big([\mathbf{v}_{F2}(\mathbf{k})]^2\text{tr}(\mathcal{G}(-\tau)\mathcal{G}(\tau)) \\ &+ [\mathbf{v}_{F1}(\mathbf{k})]^2\text{tr}(\sigma^3\mathcal{G}(-\tau)\sigma^3\mathcal{G}(\tau)) \\ &+ [\mathbf{v}_{\Delta}(\mathbf{k})]^2\text{tr}\left(\sigma^1\mathcal{G}(-\tau)\sigma^1\mathcal{G}(\tau)\right)\Big) \\ &+ (\mathbf{v}_{F1}.\mathbf{v}_{F2})\text{tr}\left((\sigma^3\mathcal{G}(-\tau) + \mathcal{G}(-\tau)\sigma^3)\mathcal{G}(\tau)\right)\Big) \\ &+ (\mathbf{v}_{F2}.\mathbf{v}_{\Delta})\text{tr}\left((\sigma^1\mathcal{G}(-\tau) + \mathcal{G}(-\tau)\sigma^1)\mathcal{G}(\tau)\right)\Big) \\ &+ (\mathbf{v}_{F1}.\mathbf{v}_{\Delta})\text{tr}\left((\sigma^1\mathcal{G}(-\tau)\sigma^3 + \sigma^3\mathcal{G}(-\tau)\sigma^1)\mathcal{G}(\tau)\right)\Big)\end{aligned} \tag{16}$$

In this equation, we have ignored vertex corrections. These are important when the scattering rate is strongly angle-dependent, as they distinguish the transport and quasiparticle lifetimes (for instance, through a $(1 - \cos\theta)$ factor) and also distinguishing umklapp scattering from momentum-conserving scattering. In what follows, we will assume that the replacement $\tau \rightarrow \tau_{\text{tr}}$ is made (*i.e.* ignore vertex corrections). Reference[18] has considered the vertex correction for DDW conductivity.

Writing $\mathcal{G}$ in terms of the spectral function $A(\mathbf{k}, \omega)$, evaluating the Matsubara sum, and doing the analytic continuation ($i\omega_n \rightarrow \omega + i\delta$), we find the optical conductivity to be[19]

$$
\begin{aligned}
\sigma(\omega) \sim \frac{1}{\omega} \sum_{RBZ} \int_{-\infty}^{\infty} \frac{d\varepsilon}{2\pi} \left[n_F(\varepsilon) - n_F(\varepsilon+\omega)\right] \times \\
\Big\{ [\mathbf{v}_{F2}(\mathbf{k})]^2 \Big[A_{11}(k,\varepsilon)A_{11}(k,\varepsilon+\omega) + 2A_{12}(k,\varepsilon)A_{12}(k,\varepsilon+\omega) + A_{22}(k,\varepsilon)A_{22}(k,\varepsilon+\omega) \Big] \\
+ [\mathbf{v}_{F1}(\mathbf{k})]^2 \Big[A_{11}(k,\varepsilon)A_{11}(k,\varepsilon+\omega) - 2A_{12}(k,\varepsilon)A_{12}(k,\varepsilon+\omega) + A_{22}(k,\varepsilon)A_{22}(k,\varepsilon+\omega) \Big] \\
+ [\mathbf{v}_{\Delta}(\mathbf{k})]^2 \Big[A_{22}(k,\varepsilon)A_{11}(k,\varepsilon+\omega) + 2A_{12}(k,\varepsilon)A_{12}(k,\varepsilon+\omega) + A_{11}(k,\varepsilon)A_{22}(k,\varepsilon+\omega) \Big] \\
+ 2\mathbf{v}_{F1}(\mathbf{k}).\mathbf{v}_{F2}(\mathbf{k}) \Big[A_{11}(k,\varepsilon)A_{11}(k,\varepsilon+\omega) - A_{22}(k,\varepsilon)A_{22}(k,\varepsilon+\omega) \Big] \\
+ 2\mathbf{v}_{F2}(\mathbf{k}).\mathbf{v}_{\Delta}(\mathbf{k}) \Big[A_{12}(k,\varepsilon)(A_{11}(k,\varepsilon+\omega) + A_{22}(k,\varepsilon+\omega)) + (A_{11}(k,\varepsilon) + A_{22}(k,\varepsilon))A_{12}(k,\varepsilon+\omega) \Big] \\
+ 2\mathbf{v}_{F1}(\mathbf{k}).\mathbf{v}_{\Delta}(\mathbf{k}) \Big[A_{12}(k,\varepsilon)(A_{11}(k,\varepsilon+\omega) - A_{22}(k,\varepsilon+\omega)) + (A_{11}(k,\varepsilon) - A_{22}(k,\varepsilon))A_{12}(k,\varepsilon+\omega) \Big] \Big\}
\end{aligned}
\tag{17}
$$

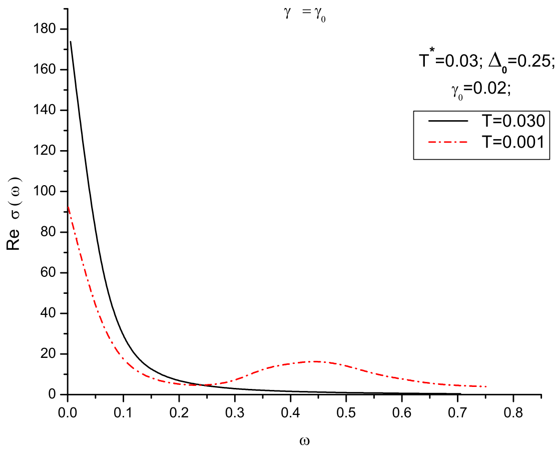

FIG. 3: Real part of the optical conductivity for a constant scattering rate $\gamma = \gamma_0 = 0.02$, $\Delta_0 = 0.25$ and $T^* = 0.030$.

where $n_F(\epsilon)$ is the Fermi distribution function. For demonstration purposes, in fig. 3 the real part of the optical conductivity has been plotted against ω for two different temperatures (one above T^*, depicted with a solid line, one below T^*, depicted with a dashed-dotted line), assuming that the quasiparticle lifetime is a constant (temperature and momentum independent) and the gap is unrealistically big ($W_0 = 0.25$ eV). As expected an upward shift of the SW occurs when the gap opens. Similar calculations have also been done in[20].

V. QUASIPARTICLE LIFETIME

Applying the formulas of the preceding section to the underdoped cuprates presupposes that the quasiparticle picture makes sense there. This is questionable, particularly in the anti-nodal regions, where even lowest-order perturbation theory around the DDW mean-field Hamiltonian[3] predicts short lifetimes which may indicate a breakdown of quasiparticles. However, we will compute the conductivity in the quasiparticle approximation to show that, even at this level, an upward shift of spectral weight is not expected. If there are no quasiparticles at the anti-nodes, then the situation may be even better.

In order to proceed with this strategy, we need one final ingredient, an *ansatz* for the quasiparticle scattering rate $1/\tau(\mathbf{k},\omega;T) = \gamma(\mathbf{k},\omega;T)$, as a function of momentum, frequency, and temperature in the underdoped cuprates. A number of angle-resolved photoemission experiments have measured the inverse lifetime (imaginary part of the self energy), as a function of these different parameters. In these experiments, the width of the quasiparticle peaks in the energy distribution curves (EDC's) or momentum distribution curve (MDC's) are measured as functions of momentum, energy and temperature[21,22,23,24]. While the transport lifetimes are not necessarily identical to the quasiparticle lifetimes (or, equivalently, the vertex corrections are not necessarily small), we expect that they will have a similar anisotropic behavior. For the purposes of this model calculation, we will simply take them to be the same. We emphasize that the lifetimes which we adopt below are for illustrative purposes since our main goal is to show that an upward movement of spectral weight is not a necessary concomitant of the emergence of DDW order at finite temperature. We are not making any claims here about the correctness of these lifetimes.

We take the imaginary part of the self-energy (quasiparticle scattering rate) to have the form

$$\Sigma_2(\mathbf{k},\omega;T) = \Sigma_2(\omega;T) + \Gamma(\mathbf{k}). \tag{18}$$

where $\Sigma_2(\omega;T)$ is temperature and frequency dependent with no momentum dependence and $\Gamma(\mathbf{k})$ is strongly momentum dependent.

Such a form has been motivated by marginal Fermi liquid phenomenology[25,26] (MFL). In this way of analyzing the data, it is assumed that the quasiparticle lifetime which comes from electron-electron scattering is independent of temperature and linear in energy for small temperatures and linear in temperature, independent of the binding energy for higher temperatures:

$$\Sigma_2^{MFL}(\omega;T) = \lambda \text{Max}(|\omega|, T). \tag{19}$$

In this *ansatz*, all of the angular dependence comes from *elastic* electron-electron scattering. This is a convenient form, but we will show that our results hold even for some others.

For instance, we repeat our calculations with the standard Fermi liquid (FL) quasiparticle lifetime:

$$\Sigma_2^{FL}(\omega;T) = \lambda \text{Max}(\omega^2, T^2). \tag{20}$$

again assuming that the angular dependence comes from $\Gamma(\mathbf{k})$. In order to show that these particular forms of ω-dependence are not playing a big role in shifts of SW, we have also tried ω-independent forms of these scattering rates: $\Sigma_2^{T-Linear}(\omega;T) = \lambda T$ and $\Sigma_2^{T^2}(\omega;T) = \lambda T^2$.

While this form of the quasiparticle lifetime does not give the correct DC conductivity, it is still useful as a check because our goal is to emphasize the role of anisotropy and show that it can lead to a downward shift of spectral weight, regardless of its detailed frequency and temperature dependence.

The quasiparticle lifetime is strongly anisotropic[23]: excitations in the antinodal region are more strongly scattered than the ones in the nodal region by up to a factor of 5. Hence, the assumed form (18) necessitates that $\Gamma(\mathbf{k})$ be a strongly anisotropic function of $\mathbf{k}$. We take the form:

$$\Gamma_{\text{Aniso}}(\mathbf{k}) = \gamma_0(1 + (\cos k_x - \cos k_y)^2), \tag{21}$$

where γ_0 is the scattering strength in the nodal region.

In order to check the role of anisotropy in the eventual shifting of the SW, we also check the case in which $\Gamma(\mathbf{k})$ is (unrealistically) isotropic:

$$\Gamma_{\text{Iso}}(\mathbf{k}) = \gamma_0. \tag{22}$$

VI. RESULTS

In Figures 4 to 7, we have plotted the real part of the optical conductivity vs ω, when the momentum-independent part of the lifetime is given by the four different forms listed above. In each figure the isotropic case is compared with the anisotropic one with the same set of parameters (listed in the figure captions) except for γ_0, which is smaller in the anisotropic case because of its extra (larger than 1) prefactor. In all cases we have $t = 0.3$, $t' = 0.09$, $\mu = -0.3$ and $T^* = 0.03$.

It is clear that in figures 4a, 5a, 6a, 7a, in which the scattering rate is isotropic, there is an upward movement of spectral weight (though it is small in some cases). However, in figures 4b, 5b, 6b, 7b, in which the scattering rate is anisotropic, there is a clear downward movement of spectral weight. (Broadening the Drude peak has also been seen in[20] and[18], in which scattering has been isotropic.)

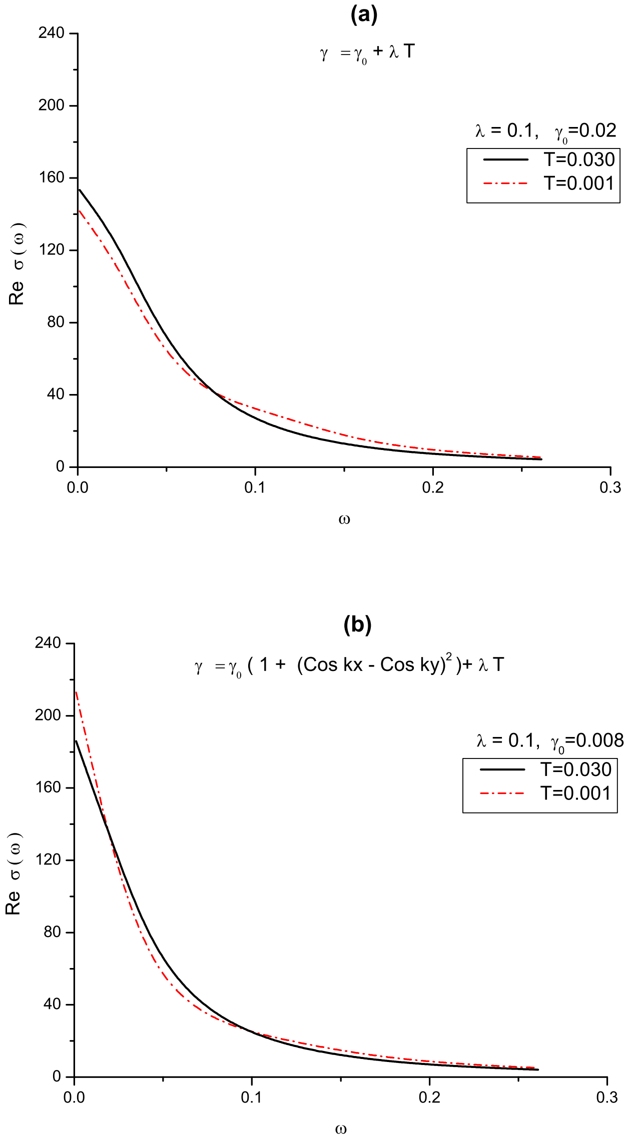

FIG. 4: Real part of the optical conductivity for (a) isotropic scattering rate with $\gamma_0 = 0.020$ and (b) anisotropic scattering rate with $\gamma_0 = 0.008$. Quasiparticle lifetime is taken to be linear in temperature and independent of ω.

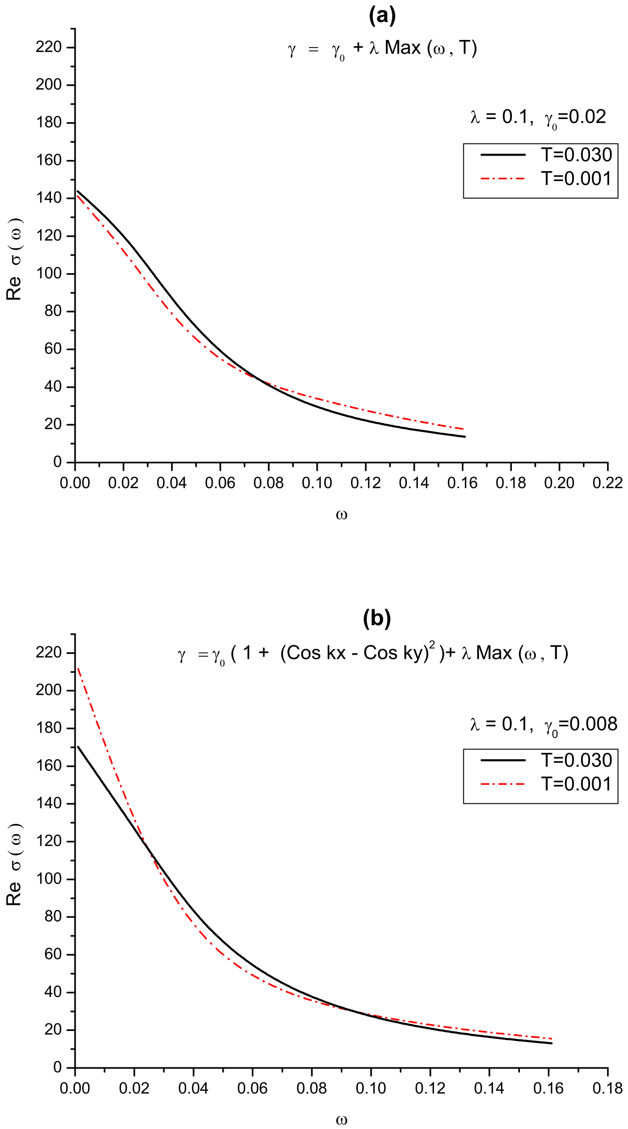

FIG. 5: Real part of the optical conductivity for (a) isotropic scattering rate with $\gamma_0 = 0.020$ and (b) anisotropic scattering rate with $\gamma_0 = 0.008$. Quasiparticle lifetime's temperature and frequency dependence is given by the marginal Fermi liquid theory.

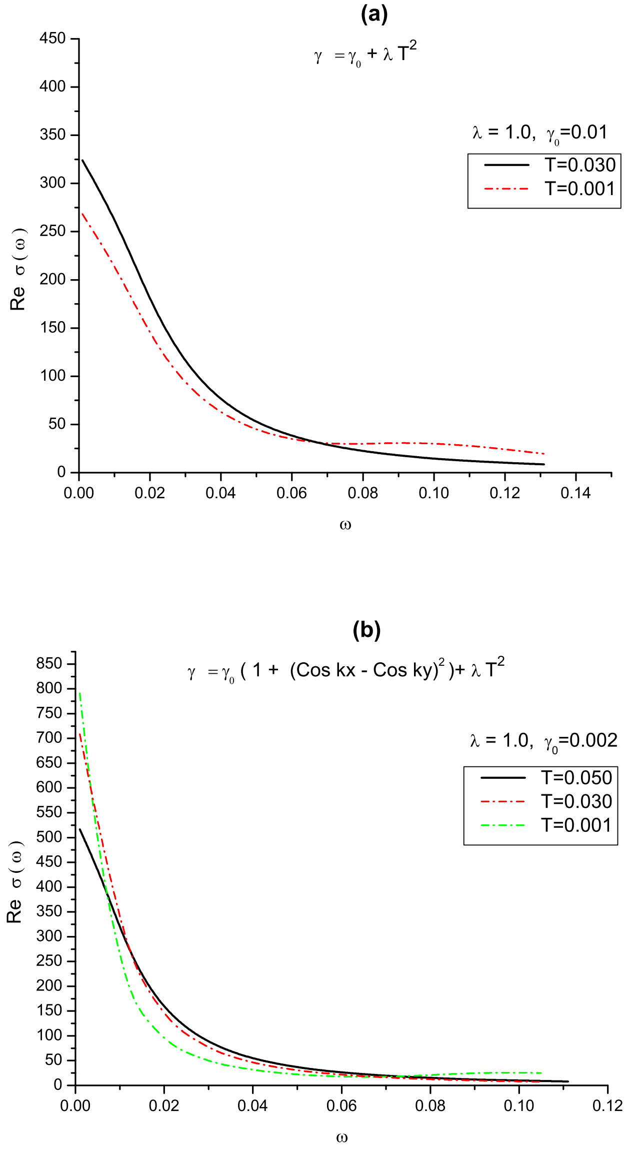

FIG. 6: Real part of the optical conductivity for (a) isotropic scattering rate with $\gamma_0 = 0.010$ and (b) anisotropic scattering rate with $\gamma_0 = 0.002$. Quasiparticle lifetime is taken be to independent of ω have a T^2 temperature dependence.

VII. CONCLUSIONS

Recent data by Santander-Syro *et al*[12], has questioned the previous belief that the opening of the pseudogap in the underdoped cuprates can be detected by in-plane optical conductivity measurements. The unexpected result that as the temperature is reduced (and although a gap opens in the antinodal region of the Brillouin zone), the spectral weight is still transferred to lower frequencies, was interpreted as lack of any pseudogap signature in the optical data. In this paper we showed that this effect is consistent with the DDW theory of the pseudogap state of the underdoped cuprates.

In the four sets of graphs of the previous section it can clearly be seen that the key factor in deciding which way the SW is transferred is isotropy or anisotropy of the scattering rate. It is shown that regardless of the form of the temperature and frequency dependence of the quasiparticle lifetime (*e.g.* Fermi liquid or non-Fermi

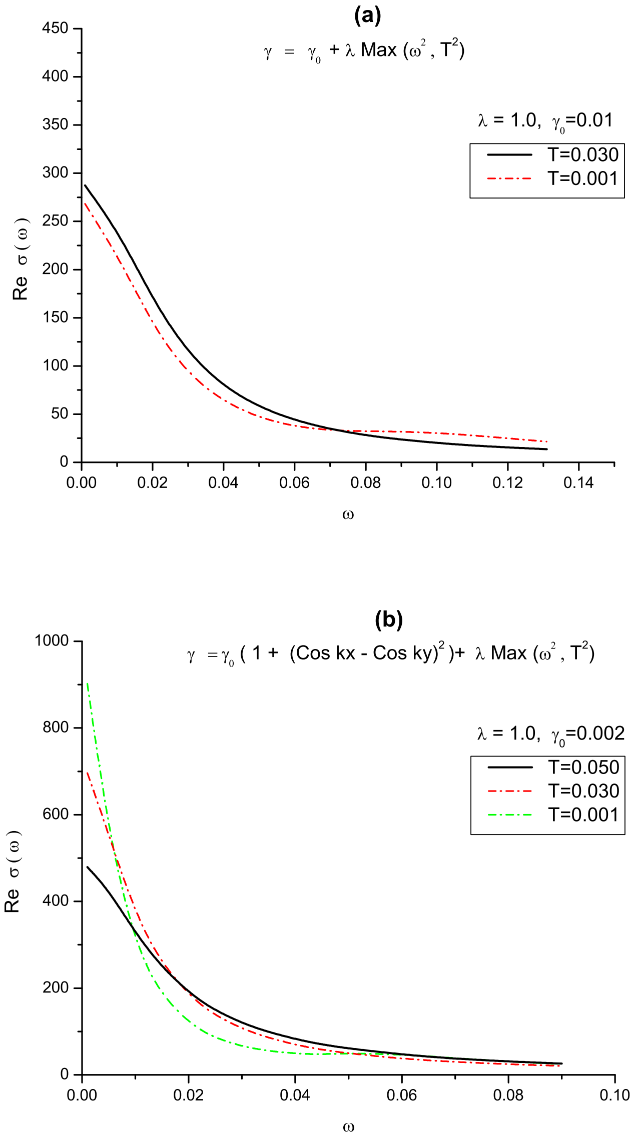

FIG. 7: Real part of the optical conductivity for (a) isotropic scattering rate with $\gamma_0 = 0.020$ and (b) anisotropic scattering rate with $\gamma_0 = 0.008$. Quasiparticle lifetime's temperature and frequency dependence is given by the Fermi liquid theory.

liquid) the SW is shifted upward for the isotropic scattering rate while it is shifted downward for the anisotropic case. (We have not tried to find a form for the quasiparticle lifetime which correctly reproduces all of the transport data, but have focussed on the role of anisotropy and have shown that similar results are obtained for several different forms of frequency and temperature dependence.)

We believe the explanation to be as follows: the pseudogap opens in the antinodal region where the carriers are more strongly scattered than the ones in the nodal region, where there is no gap. Therefore, we have lost those excitations which already gave relatively little contribution to the transport properties of the normal state. Furthermore, by reducing the temperature, the scattering rate of all the excitations is reduced. Our results clearly show that in the (more realistic) anisotropic case, the effect of lost excitations due to the gap opening can be more than canceled by a temperature-dependent reduction of the scattering rate for the rest of the excitations and hence a downward shift of the optical spectral weight. It is obvious that anisotropy is the key here, since for similar parameters for isotropic scattering rate, an upward transfer is observed. We note that similar considerations should apply to the case of 2H-TaSe$_2$[28].

Acknowledgments

We would like to thank Sudip Chakravarty and Dmitri Basov for discussions. This work has been supported by the NSF under Grant No. DMR-0411800.

---

[1] S. Chakravarty, R. B. Laughlin, D. K. Morr and C. Nayak , Phys. Rev. B **63**, 094503 (2001).

[2] C. Nayak, Phys. Rev. B **62**, 4880 (2000), **62** R6134 (2000).

[3] S. Chakravarty, C. Nayak and S. Tewari, Phys. Rev. B **68**, 100504(R) (2003).

[4] S. Tewari, H. -Y. Kee, C. Nayak and S. Chakravarty, Phys. Rev. B **68**, 100504(R) (2003).

[5] S. Tewari, S. Chakravarty, J. Fjærestad, C. Nayak and R. S. Thompson, Phys. Rev. B **70**, 014514 (2004).

[6] C. Bena, S. Chakravarty, J. Hu and C. Nayak, Phys. Rev. B **69**, 134517 (2004).

[7] S. Chakravarty, C. Nayak, S. Tewari and X. Yang, Phys. Rev. Lett. **89**, 277003 (2002).

[8] L. Benfatto, S.G. Sharapov,N. Andrenacci and H. Beck, Phys. Rev. B **71**, 104511 (2005).

[9] L. Benfatto, S.G. Sharapov and H. Beck, Eur. Phys. J. B **39**, 169 (2004).

[10] H. A. Mook, Pengcheng Dai, S. M. Hayden, A. Hiess, J. W.

Lynn, S. -H. Lee, and F. Dogan, Phys. Rev. B **66**, 144513 (2002).

[11] G. Grüner, *Density Waves in Solids*, Adison Wesley, New York, 1994, and references therein.

[12] A.F. Santander-Syro, R.P.S.M. Lobo, N.Bontemps, Z. Konstantinovic, Z. Li and H. Raffy, Phys. Rev. Lett. **88**, 097005 (2002).

[13] A.V. Puchkov, D. N. Basov, and T. Timusk, J. Phys. Condens. Matter **8**, 10 049 (1996).

[14] T. Timusk and B. Statt, Rep. Prog. Phys. **62**, 61 (1999).

[15] D. N. Basov, E. J. Singley, and S. V. Dordevic, Phys. Rev. B **65**, 054516 (2002).

[16] B. P. Stojkovic and D. Pines, Phys. Rev. B **55**, 8576-8595 (1997).

[17] L. B. Ioffe and A. J. Millis, Phys. Rev. B **58**, 11631-11637 (1998).

[18] D. N. Aristov and R. Zeyher, Phys. Rev. B **71**, 104511 (2005).

[19] G. D. Mahan, *Many Paricle Physics* (Plenum, New York, 1981).

[20] B. Valenzuela, E.J. Nicol, J.P. Carbotte, Phys. Rev. B **71**, 134503 (2005).

[21] T. Valla, A.V. Fedorov, P. D. Johnson, Q. Li, G. D. Gu, and N. Koshizuka, Phys. Rev. Lett. **85**, 828 (2000).

[22] T. Valla, A. V. Fedorov, P. D. Johnson, B. O. Wells, S. L. Hulbert, Q. Li, G. D. Gu, N. Koshizuka, Science **285**, 2110 (1999).

[23] A. Kaminski et al., cond-mat/0404385.

[24] A. Kaminski et al., Phys. Rev. Lett. **84**, 1788 (2000).

[25] C. M. Varma, P. B. Littlewood, S. Schmitt-Rink, E. Abrahams and A. E. Ruckenstein, Phys. Rev. Lett. **63**, 1996 (1989).

[26] E. Abrahams and C. M. Varma, Proc. Natl. Acad. Sci. USA , **97**, 5714.

[27] G. Rickayzen, *Green's Functions and Condensed Matter Physics* (Academic Press, London, 1980).

[28] V. Vescoli, L. Degiorgi, H. Berger, and L. Forró Phys. Rev. Lett. **81**, 453-456 (1998)